

# Two-photon ionization of the $K$ -shell of an atomic ion

© A.N. Hopersky, A.M. Nadolinsky<sup>✉</sup>, R.V. Koneev

Rostov State University for Railway Transportation, Rostov-on-Don, Russia

<sup>✉</sup>e-mail: amnrnd@mail.ru

Received April 03, 2025

Revised June 08, 2025

Accepted June 27, 2025

Theoretical predictions of the analytical structure and absolute values of the generalized cross section of two-photon single ionization of the  $K$ -shell of the heavy neon-like atomic ion of iron ( $\text{Fe}^{16+}$ ) are presented. A pronounced resonance subthreshold structure of the generalized cross section and the effect of destructive quantum interference of probability amplitudes of radiative transitions into virtual excited states of  $p$ -symmetry are established. The presence of a valence  $2p^6$ -shell in the ionic core leads to the emergence of an additional giant resonance in the generalized cross section as an effect of "inverse" hard x-ray emission of the  $K_\alpha$ -type  $1s^2(2s^2)2p^5 + \hbar\omega \rightarrow 1s(2s^2)2p^6$ . A scheme of the proposed experiment with linearly polarized x-ray photons to verify the obtained theoretical results is presented.

**Keywords:** two-photon resonant single ionization, neon-like atomic ion, probability amplitude, generalized cross section.

DOI: 10.61011/EOS.2025.07.61898.7780-25

## 1. Introduction

The creation of an x-ray free-electron laser (XFEL) as a source of hard x-ray radiation has opened the possibility for high-precision experimental and theoretical studies of one of the fundamental processes in the microscopic world — the two-photon (nonlinear) single ionization of deep atomic shells of atoms, atomic ions, molecules, and solids [1,2]. Studies of this process have revealed, in particular, the important roles of (a) relativistic effects and screening effects in the nonresonant generalized cross section of two-photon ionization of the  $K$ -shell of an atom [3] and (b) nondipole (quadrupole) effects in the angular distribution of photoelectrons generated by above-threshold two-photon ionization of the  $K$ -shell of an atom [4]. In the cited works, to our knowledge, there are no studies of the resonant subthreshold structure of the generalized cross section of two-photon ionization. In the authors' previous works [5–7], within the second order of nonrelativistic quantum perturbation theory, the first theoretical studies of the generalized cross section of two-photon resonant single ionization of the  $1s^2$ -shell of atoms (Ne, Ar), beryllium-like ( $\text{Ne}^{6+}$ ) and helium-like ( $\text{Ne}^{8+}$ ) atomic ions were carried out, considering only the main (leading in the infinite complete set) part of the subthreshold resonant structure of the cross sections and effects of radial relaxation of the transition states in the field of the  $1s$ -vacancy. The theory of works [5–7] is generalized in this article to heavy neon-like atomic ions and modified to account for (a) completeness of the set of virtual (intermediate) photonic excitation states, (b) nontrivial angular structure of probability amplitude transitions into final states of  $d$ -symmetry, and (c) destructive quantum interference of partial probability amplitude transitions. The object of study is the neon-like ion of

the iron atom ( $\text{Fe}^{16+}$ , ionic nuclear charge  $Z = 26$ , ground state configuration  $[0] = 1s^2 2s^2 2p^6 [^1S_0]$ ). The choice is motivated by the spherical symmetry of the ground state of ion  $\text{Fe}^{16+}$ , its availability in gas phase [8] for experiments on absorption of two linearly polarized XFEL photons with energy  $\hbar\omega$  ( $\hbar$  — Planck constant,  $\omega$  — photon circular frequency) by an ion trapped in a „trap“ [9] and the demand for its spectral characteristics in astrophysics [10].

## 2. Theory

The probability amplitudes and generalized cross section for two-photon ionization are obtained in the leading second order (in the number of interaction vertices) of nonrelativistic quantum perturbation theory. In the structure of the radiation transition operator,

$$\hat{R} = -\frac{1}{c} \sum_{n=1}^N (\hat{p}_n \cdot \hat{A}_n), \quad (1)$$

for the electromagnetic field operator (in the second quantization representation), the dipole approximation is adopted:

$$\hat{A}_n \rightarrow \sum_{\mathbf{k}} \sum_{\rho=1,2} \mathbf{e}_{\mathbf{k}\rho} (\hat{a}_{\mathbf{k}\rho}^+ + \hat{a}_{\mathbf{k}\rho}^-), \quad (2)$$

$$(\mathbf{k} \cdot \mathbf{r}_n) \ll 1 \Rightarrow \exp\{\pm i(\mathbf{k} \cdot \mathbf{r}_n)\} \cong 1. \quad (3)$$

The criterion of applicability of the dipole approximation in the form  $\theta_{nl} = \lambda_\omega / r_{nl} \gg 1$  (where  $\lambda_\omega$  is the wavelength of the absorbed photon,  $r_{nl}$  is the average radius of the  $nl$ -shell of the ion) for the  $\text{Fe}^{16+}$  ion at photon absorption energies  $\hbar\omega = 8$  (6.4) keV is  $\theta_{1s}(\theta_{2p}) \cong 50$  (16). Here, the values  $r_{1s}(r_{2p}) = 0.031$  (0.123) Å (this work's calculation) are used. In relations (1)–(3)  $e(m_e)$  is the electron charge

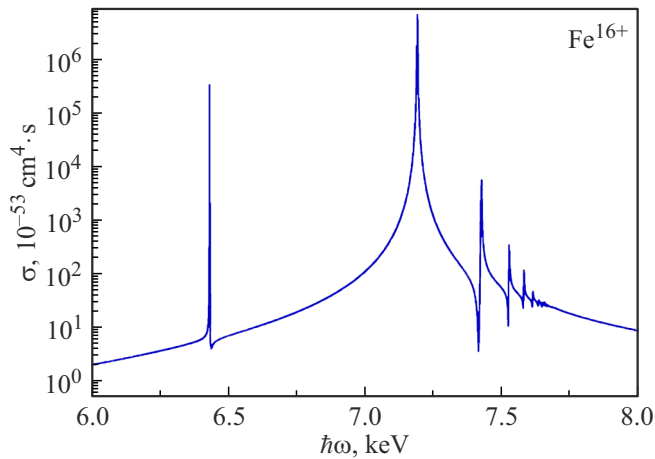


**Figure 1.** Total generalized cross section of two-photon resonant single ionization of the  $K$ -shell of the  $\text{Fe}^{16+}$  ion,  $\hbar\omega$  — energy of the absorbed photon.

**Table 1.** Spectral characteristics of leading resonances  $1s \rightarrow np$  of the generalized cross section of two-photon single ionization of the  $K$ -shell of the  $\text{Fe}^{16+}$  ion in the photon energy region  $\hbar\omega \in (7.00; 7.70)$  keV,  $[n] \equiv 10^n$  notation introduced

np	$I_{1snp}$ , keV	$\sigma_g$ , $10^{-53} \text{ cm}^4 \cdot \text{s}$
3p	7.194	$6.55 \cdot [6]$
4p	7.427	$5.52 \cdot [3]$
5p	7.529	$3.48 \cdot [2]$
6p	7.583	$1.19 \cdot [2]$

**Table 2.** Relative contributions of  $s$ - and  $d$ -symmetries of the final ionization state  $\Lambda = \sigma_g^{(d)}/\sigma_g^{(s)}$  (see (28) for terms  $l = d$  and  $l = s$ ) into the total generalized cross section of two-photon resonant single ionization of the  $K$ -shell of the  $\text{Fe}^{16+}$  ion

$\hbar\omega$ , keV	6.0	7.0	8.0
$\Lambda$	2.504	2.573	2.660

(mass),  $c$  is the speed of light in vacuum,  $N$  is the number of electrons in the ion,  $\hat{p}_n(\mathbf{r}_n)$  is the momentum (position) operator of the  $n$ -electron of the ion,  $\mathbf{e}_{\mathbf{k}\rho}(\mathbf{k})$  is the polarization vector (wave vector) of the photon, and  $\hat{a}_{\mathbf{k}\rho}^+$  ( $\hat{a}_{\mathbf{k}\rho}^-$ ) is the photon creation (annihilation) operator.

Consider the following channels of two-photon single ionization of the  $K$ -shell of a neon-like atomic ion:

$$2\omega + [0] \rightarrow 2p^5 x l + \omega \rightarrow 1s \varepsilon l, \quad (4)$$

$$2\omega + [0] \rightarrow 1s(n, x)p + \omega \rightarrow 1s \varepsilon l. \quad (5)$$

In (1), (4), (5) and below, atomic units are adopted ( $e = \hbar = m_e = 1$ ),  $x(\varepsilon)$  is the energy of the continuous

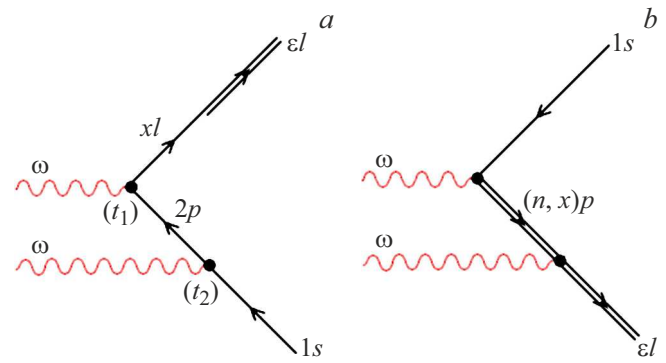


**Figure 2.** Probability amplitudes of two-photon resonant single ionization of the  $K$ -shell of a neon-like atomic ion in Feynman diagram representation: (a) via channel (4), (b) via channel (5). Time direction is left to right ( $t_1 < t_2$ ). Arrow to the right indicates electron, arrow to the left indicates vacancy. Double line indicates state obtained in Hartree-Fock field of  $1s$  vacancy. The connection of single and double lines corresponds to overlap integral  $\langle x l | \varepsilon l \rangle$ ,  $l = s, d$ . The black dot represents the vertex of the radiative transition,  $\omega$  is the absorbed photon.

spectrum electron,  $n$  is the principal quantum number of the excited discrete spectrum state,  $l = s, d$  and the occupied electron shells of the ion's configuration are not indicated. In the calculation results (Fig. 1, Tables 1, 2), conventional units are restored through Planck's constant. Intermediate  $2p^5 n l$  discrete spectrum states at  $\omega \gg I_{2pnl}$  ( $I_{2pnl}$  is the energy of photoexcitation  $2p \rightarrow n l$ ) omitted in (4) are suppressed by the energy denominator  $(\omega - I_{2pnl} + i\gamma_{2p})^{-1}$  (here,  $\gamma_{2p} = \Gamma_{2p}/2$ ,  $\Gamma_{2p}$  are widths of decay of the  $2p$ -vacancy) and by the smallness of the overlap integral  $\langle n l | \varepsilon l \rangle \ll 1$  in the probability amplitude of two-photon ionization. The strong spatial and energetic separation of the subvalence ( $2s^2$ ) and valence ( $2p^6$ ) shells from the deep  $1s^2$  shell of the  $\text{Fe}^{16+}$  ion allows neglecting production of final  $2s \varepsilon(s, d)$ - and  $2p^5 \varepsilon(p, f)$ -states of two-photon ionization. Indeed, for the  $\text{Fe}^{16+}$  ion, the inequalities are satisfied:  $r_{1s} = 0.031 \text{ \AA} \ll r_{2s}(r_{2p}) = 0.140(0.123) \text{ \AA}$ ,  $I_{1s} = 7699.23 \text{ eV}$  (this work's relativistic calculation  $\gg I_{2s}(I_{2p}) = 1397.77(1270.60) \text{ eV}$  [11],  $I_{nl}$  is the ionization threshold energy of the  $nl$ -shell of the ion. Finally, the amplitude of two-photon ionization via the  $2\omega + [0] \rightarrow 1s \varepsilon l$  channel is determined by the contact interaction operator  $\hat{C} = (1/2c^2) \sum_{n=1}^N (\hat{A}_n \cdot \hat{A}_n)$  and is proportional to the matrix element  $\langle 1s | j_i | \varepsilon \rangle$ , where  $j_i$  is the spherical Bessel function. In the dipole approximation for the  $\hat{A}_n$ -operator  $j_0 \rightarrow 1$ ,  $j_2 \rightarrow 0$  and  $\langle 1s | j_i | \varepsilon l \rangle \rightarrow 0$ .

Probability amplitudes of two-photon ionization via channels (4) and (5) are physically interpreted in Fig. 2 in the formalism of (nonrelativistic) Feynman diagrams. We establish their analytical structure.

## 2.1. Amplitude via channel (4)

According to Fig. 2, *a*, for the sought amplitudes we have the following expressions:

$$A_l = \sum_{M'} \int_0^\infty dx \frac{\langle 0 | \hat{R} | \Phi_{xl} \rangle \langle \Phi_{xl} | \hat{R} | \Psi_{el} \rangle}{\omega - I_{2p} - x + i\gamma_{2p}}, \quad (6)$$

$$|0\rangle = [0] \otimes (\hat{a}_\omega^+)^2 |0_{ph}\rangle, \quad (7)$$

$$|\Phi_{xl}\rangle = |2p^5 x l ({}^1P_1), M'\rangle \otimes \hat{a}_\omega^+ |0_{ph}\rangle, \quad (8)$$

$$|\Psi_{el}\rangle = |1s \varepsilon l ({}^1L_{J=l}), M\rangle \otimes |0_{ph}\rangle. \quad (9)$$

In (6)–(9) the full wave functions of the initial ( $|0\rangle$ ), intermediate ( $|\Phi\rangle$ ) and final ( $|\Psi\rangle$ ) states of two-photon ionization are defined, projections of total moments of the „ion residual  $\otimes$  electron„ system  $M' = 0, \pm 1, M = 0$  for  $l = s, M = 0, \pm 1, \pm 2$  for  $l = d$  and  $|0_{ph}\rangle$  is the photon vacuum wave function of quantum electrodynamics. The structure of the  ${}^1L_{J=l}$  terms of the final states of two-photon ionization ( $J = 0 \Rightarrow {}^1S_0; J = 2 \Rightarrow {}^1D_2$ ) reproduces the Landau-Yang theorem [12,13] for the total momentum of the system of two absorbed photons  $J_\omega = 0, 2$ . Using methods of photon creation (annihilation) operator algebra, theories of irreducible tensor operators, theory of nonorthogonal orbitals [14], and the approximation (states obtained in different self-consistent fields, Fig. 2, *a*) for the overlap integral of continuum spectrum wavefunctions  $\langle x l | \varepsilon l \rangle \cong \delta(x - \varepsilon)$  (here  $\delta$  is the Dirac delta function), from (6) we obtain:

$$A_s = \xi \langle 2p_0 | \hat{r} | \bar{\varepsilon} s_+ \rangle, \quad (10)$$

$$A_d = \sqrt{6} \xi \langle 2p_0 | \hat{r} | \bar{\varepsilon} d_+ \rangle Q_M, \quad (11)$$

$$\xi = \frac{4\pi}{3V\omega} \frac{\omega_{sp}(2\omega - \omega_{sp})}{(\omega - \omega_{sp} - i\gamma_{2p})} \langle 1s_0 | \hat{r} | 2p_+ \rangle, \quad (12)$$

$$Q_M = -\frac{4\pi}{3} \sum_{M'} \sum_p (-1)^{M'} Y_{1,M'}(\mathbf{e}_\omega) Y_{1,p}^*(\mathbf{e}_\omega) \times \begin{pmatrix} 1 & 1 & 2 \\ -M' & p & M \end{pmatrix}. \quad (13)$$

Here,  $\bar{\varepsilon} = 2\omega - I_{1s}$ ,  $\omega_{sp} = I_{1s} - I_{2p}$ ,  $V(\text{cm}^3) = c$  are the quantization volume of the electromagnetic field (numerically equal to the speed of light in vacuum) [15],  $Y_{\alpha,\beta}(\mathbf{e}_\omega)$  is the spherical function,  $p = 0 \pm 1$ , „\*“ is the complex conjugation symbol and the  $3j$ -Wigner symbol is defined. In equations (10)–(12) „0“ and „+“ indices correspond to the radial parts of electronic wavefunctions obtained by solving single-configuration Hartree-Fock self-consistent field equations for the  $[0]$ - and  $1s_+ \varepsilon l_+$ -configurations of the ion. The appearance of the multiplier  $Q_M$  in (11) reflects the fact of the nontrivial angular structure of the probability amplitude of transition to final states of  $d$ -symmetry (in the upper line of the  $3j$ -Wigner symbol  $J = 2$ ).

## 2.2. Amplitude via channel (5)

According to Fig. 2, *b*, for the sought amplitudes we have quantum interference of partial amplitudes:

$$B_l = B_l^{(1)} + B_l^{(2)}, \quad (14)$$

$$B_l^{(1)} = \sum_{M'} \sum_{n=3}^\infty \frac{\langle 0 | \hat{R} | K_n \rangle \langle K_n | \hat{R} | \Psi_{el} \rangle}{\omega - I_{1snp} + i\gamma_{1s}}, \quad (15)$$

$$B_l^{(2)} = \sum_{M'} \int_0^\infty dx \frac{\langle 0 | \hat{R} | K_x \rangle \langle K_x | \hat{R} | \Psi_{el} \rangle}{\omega - I_{1s} - x + i\gamma_{1s}}, \quad (16)$$

$$|K_{n,x}\rangle = |1s(n, x)p({}^1P_1), M'\rangle \otimes \hat{a}_\omega^+ |0_{ph}\rangle, \quad (17)$$

where  $I_{1snp}$  is the energy of photoexcitation  $1s \rightarrow np$ ,  $\gamma_{1s} = \Gamma_{1s}/2$  and  $\Gamma_{1s}$  are the decay widths of the  $1s$  vacancy. For the denominator of the probability amplitude (15), the approximation of independence of the parameter  $\Gamma_{1s}$  from the principal quantum number of the photoexcited state  $1s \rightarrow np$  is adopted. Following the methods of constructing  $A_l$  amplitudes of Section 2.1 and the plane wave approximation  $|x(r)\rangle \sim \sin(r\sqrt{2x})$  for the one-electron probability amplitude of radiative transition between continuum states in (16),

$$(x - \varepsilon) \langle x p_+ | \hat{r} | \varepsilon l_+ \rangle \cong i\sqrt{2x} \delta(x - \varepsilon), \quad (18)$$

for (14) we obtain:

$$B_s = \eta(\mu + \sum_{n=3}^\infty \beta_n \langle np_+ | \hat{r} | \bar{\varepsilon} s_+ \rangle), \quad (19)$$

$$B_d = \sqrt{6} \cdot \eta(\mu + \sum_{n=3}^\infty \beta_n \langle np_+ | \hat{r} | \bar{\varepsilon} d_+ \rangle) Q_M, \quad (20)$$

$$\mu = i2\sqrt{2\varepsilon} \langle 1s_0 \| \hat{r} \| \bar{\varepsilon} p_+ \rangle, \quad (21)$$

$$\beta_n = \frac{I_{1snp}(2\omega - I_{1snp})}{(\omega - I_{1snp} + i\gamma_{1s})} \langle 1s_0 \| \hat{r} \| np_+ \rangle, \quad (22)$$

where  $\eta = \frac{4\pi}{3} \frac{1}{V\omega}$  and the one-electron probability amplitude of photoexcitation  $1s \rightarrow np$  is defined (taking into account radial relaxation of core and excited states in the Hartree-Fock field of the  $1s$ -vacancy by the methods of the theory of nonorthogonal orbitals):

$$\langle 1s_0 \| \hat{r} \| np_+ \rangle = N_{1s} (\langle 1s_0 | \hat{r} | np_+ \rangle - F_n), \quad (23)$$

$$N_{1s} = \langle 1s_0 | 1s_+ \rangle \langle 2s_0 | 2s_+ \rangle^2 \langle 2p_0 | 2p_+ \rangle^6 \quad (24)$$

$$F_n = \frac{\langle 1s_0 | \hat{r} | 2p_+ \rangle \langle 2p_0 | np_+ \rangle}{\langle 2p_0 | 2p_+ \rangle}. \quad (25)$$

### 2.3. Generalized cross section of ionization

Following the definition of the notion of generalized cross section of two-photon single ionization of an atom (atomic ion) [16],

$$d\sigma_g^{(l)} = (V/2c)d\sigma_l, \quad (26)$$

taking into account the quantum interference of  $A_l$  and  $B_l$  amplitudes in Fermi's „golden rule“ [17],

$$d\sigma_l = (\pi V/c)|A_l + B_l|^2 \delta(\varepsilon - \bar{\varepsilon}) d\varepsilon, \quad (27)$$

and integrating in (27) over the photoelectron energy, for the sought total generalized cross section we obtain (the probability of photon disappearance without photoelectron registration):

$$\sigma_g = \chi \frac{1}{\omega^2} \sum_{l=s,d} \sum_{i=1,2} a_l L_{il}^2, \quad (28)$$

$$L_{1l} = (\omega - \omega_{sp})L_l + \sum_{n=3}^{\infty} (\omega - I_{1snp})C_{ln}, \quad (29)$$

$$L_{2l} = \gamma_{2p}L_l - \gamma_{1s} \sum_{n=3}^{\infty} C_{ln} + D, \quad (30)$$

$$L_l = \frac{\omega_{sp}(2\omega - \omega_{sp})}{(\omega - \omega_{sp})^2 + \gamma_{2p}} \langle 1s_0 | \hat{r} | 2p_+ \rangle \langle 2p_0 | \hat{r} | \bar{\varepsilon} l_+ \rangle, \quad (31)$$

$$C_{ln} = \frac{I_{1snp}(2\omega - I_{1snp})}{(\omega - I_{1snp})^2 + \gamma_{1s}^2} \langle 1s_0 \| \hat{r} \| np_+ \rangle \langle np_+ | \hat{r} | \bar{\varepsilon} l_+ \rangle, \quad (32)$$

$$D = 2\sqrt{2\bar{\varepsilon}} \langle 1s_0 \| \hat{r} \| \bar{\varepsilon} p_+ \rangle, \quad (33)$$

where  $\chi = 0.278 \cdot 10^{-52} \text{ cm}^4 \cdot \text{s}$ ,  $a_s = 1$ ,  $a_d = \frac{3}{2} a_d^{(0)} \left(1 - \frac{1}{4\pi}\right)$  and  $a_d^{(0)} = 4/5$  [5–7] (only the  $M = 0$  projection of the total moment  $J = 2$ ) is taken into account). When calculating the coefficient

$$a_d = 6 \sum_{M=-2}^2 |Q_M|^2 \quad (34)$$

in the sum of squared probability amplitudes of transitions over  $M$  projections of final states of  $d$ -symmetry, the analytical result of work [18] for the sum of products of  $3j$  Wigner symbols (Appendix) is taken into account and the scheme of the proposed XFEL experiment for linearly polarized absorbed photons is implemented:  $\mathbf{k} \in OZ$ ,  $\mathbf{e}_\omega \in OX$  ( $OX$ ,  $OZ$  are the axes of an orthogonal coordinate system)  $\Rightarrow$

$$Y_{1,0}(\mathbf{e}_\omega) = 0, \quad Y_{1,\pm 1}(\mathbf{e}_\omega) = \mp 3/(4\pi\sqrt{2}). \quad (35)$$

According to (34), the additional accounting for ( $a_d^{(0)} \rightarrow a_d$ ) projections  $M = \pm 1, \pm 2$  of the total moment  $J = 2$  significantly (by  $\sim 30\%$ ) increases the contribution of the component of the generalized cross section (28) for  $l = d$ .

### 3. Results and discussion

Calculation results are presented in Fig. 1 and Tables 1, 2. For the parameters of the generalized cross section (28), values of  $\Gamma_{1s} = 1.046 \text{ eV}$  [19],  $\Gamma_{2p} = 0.023 \text{ eV}$  (extrapolation of data from works [20,21] for radiative decay widths  $2p^5 n(s, d) \rightarrow 2p^6$ ,  $n \in [3; \infty)$ ),  $I_{1s} = 7699.23 \text{ eV}$ ,  $I_{2p} = 1270.60 \text{ eV}$  [11] and  $\omega \in (6; 8) \text{ keV}$  ([22] LCLS XFEL, USA; [23] PAL-XFEL, Republic of Korea; [24] European XFEL, Germany).

Results in Fig. 1 and Table 1 demonstrate a pronounced subthreshold resonant structure of the generalized cross section of two-photon ionization of the  $\text{Fe}^{16+}$  ion at  $\omega \in (6.25; 7.70) \text{ keV}$ . The cross section structure at  $\omega \in (7.00; 7.70) \text{ keV}$  is due to virtual photoexcitation states  $1s \rightarrow np$  (Fig. 2,  $b$ ; principal quantum number values  $n \in [3; 150]$  taken into account). The giant resonance of the generalized cross section at  $\omega = 6.4329 \text{ keV}$  is caused by radiative absorption of the  $1s^2 2p^5 + \omega \rightarrow 1s 2p^6$  second incident photon on the ion (Fig. 2,  $a$ ). Its value  $\sigma_g \cong 2 \cdot 10^{-48} \text{ cm}^4 \cdot \text{s}$  is almost an order of magnitude smaller than the leading resonance value of photoexcitation  $1s \rightarrow 3p$  but significantly exceeds photoexcitation resonance values  $1s \rightarrow np$  for  $n \geq 4$  (Table 1).

Results in Fig. 1 also demonstrate the effect of destructive (canceling) quantum interference of probability amplitudes of resonance transition states  $1s^2 2p^5 \rightarrow 1s 2p^6$  and  $1s \rightarrow np$ . This effect is caused by the alternating sign of the factors  $(\omega - \omega_{sp})$  and  $\omega - I_{1snp}$  in (29) and the „immersion“ of these states in the continuum ( $D$  in (30)). Between resonance maxima of the generalized cross section, „transparency windows“ arise in the form of sharp drops in the probability of two-photon ionization of the  $\text{Fe}^{16+}$ .

Formally, mathematically infinite sums in (29), (30) correspond to taking into account the completeness of the set of virtual photoexcitation states  $1s \rightarrow np$ . For hydrogen-like ions, the method of analytical summation of such series was proposed in work [25]. Another effective approach to the problem of accounting for completeness of the set is substituting summation of series with minimization of the functional of matrix elements of transitions (the stable variation method), realized in works [26–28]. However, to our knowledge, the problem of analytical accounting for completeness of the set in many-electron systems remains open. In this work, the numerical summation method of authors [29] is implemented. Values of  $I_{1snp}$  and  $J_n = \langle 1s_0 \| \hat{r} \| np_+ \rangle$  for  $n \in [3; 10]$  were obtained in the single-configuration Hartree-Fock approximation. For  $n \in [11; \infty)$  photoexcitation energies  $1s \rightarrow np$  were obtained by approximation of the form

$$I_{1snp} = I_{1s} - \frac{1}{n^2} \left( a - \frac{b}{n} \right), \quad \lim_{n \rightarrow \infty} I_{1snp} = I_{1s}, \quad (36)$$

where quantities  $a$  and  $b$  are defined by values  $I_{1smp}$  for  $m = 9, 10$ . For  $n \in [11; \infty)$  photoexcitation amplitudes

$1s \rightarrow np$  were obtained by approximation of the form

$$J_n = \frac{1}{n^2} \left( c + \frac{d}{n} + \frac{f}{n^2} \right), \quad \lim_{n \rightarrow \infty} J_n = 0, \quad (37)$$

where quantities  $c$ ,  $d$  and  $f$  are defined by values  $J_m$  for  $m = 8, 9, 10$ . For the integral in (32), formula (37) is implemented, considering the fact that quantities  $c$ ,  $d$  and  $f$  become functions of the absorbed photon energy ( $\bar{\epsilon} = 2\omega - I_s$ ).

As expected, due to inequalities for one-electron probability amplitudes of transitions in (31) and (32),

$$|\langle 2p_0(np_+) | \hat{r} | \bar{\epsilon} d_+ \rangle| > |\langle 2p_0(np_+) | \hat{r} | \bar{\epsilon} s_+ \rangle|, \quad (38)$$

results in Table 2 show the leading role of  $d$ -symmetry of the final ionization state in determining the value of the total generalized cross section at  $\omega \in (6; 8)$  keV. A similar assertion (on the example of ionization of the *K*-shell of neutral atoms Ne and Ge) about the leading role of the  $s \rightarrow p \rightarrow d$  two-photon ionization channel over the  $s \rightarrow p \rightarrow s$  channel is given in [3]. Thus, in single ionization of the *K*-shell of a neon-like atomic ion by two photons, the most probable realization corresponds to the total photon system moment  $J_\omega = 2$ . This result is analogous to that for one-photon ( $J_\omega = 1$ ) single ionization of the *n**l*-shell of an atom (atomic ion), where the transition  $l \rightarrow l + 1$  is called the „main“ one [30].

## 4. Conclusion

A nonrelativistic version of the quantum theory of the process of two-photon resonant single ionization of the *K*-shell of a heavy neon-like atomic ion is constructed. The effects of (a) emergence of giant resonances in the subthreshold region of the generalized ionization cross section, (b) destructive quantum interference of partial probability amplitudes of transitions, and (c) the leading role of  $d$ -symmetry of the final ionization state in determining the total generalized cross section in the hard x-ray photon energy region  $\omega \in (6; 8)$  keV are established. Going beyond the dipole approximation for the *R*-radiation transition operator and accounting for correlation and relativistic effects are the subjects of future theoretical development. Generalization of the presented theory to atoms and atomic ions of other types and establishing the role of their nuclear charge are subjects of future investigation. Finally, results of successful experiments observing two-photon ionization of atoms, molecules, and solids [1,2] allow us to suppose that absolute values of the generalized cross section in Fig. 1 are quite accessible for measurement in modern XFEL experiments. It is interesting to note that the „analogue“ of two-photon single ionization of an atom (atomic ion) in quantum electrodynamics — the linear Breit-Wheeler effect (production of an electron-positron pair by two real  $\gamma$ -quanta:  $\gamma\gamma \rightarrow e^+e^-$ ) [31] has not yet been experimentally unequivocally identified [32]. However, this effect is experimentally registered through production of two

virtual  $\gamma$ -quanta in peripheral collisions of heavy gold ions (Au;  $Z = 79$ ) [33] and lead (Pb;  $Z = 82$ ) [34].

## Appendix

Expression (34) contains the sum of products of Wigner-symbols of the form

$$W_{cd}^{ab} = \sum_{m=-2}^2 \begin{pmatrix} 1 & 1 & 2 \\ a & b & m \end{pmatrix} \begin{pmatrix} 1 & 1 & 2 \\ c & d & m \end{pmatrix}. \quad (A1)$$

The result of the analytical summation in (A1) was established in work [18]. Here we briefly reproduce it.

Consider the orthogonality condition of  $3j$ -Wigner symbols [35]:

$$\sum_j \sum_m (2j+1) \begin{pmatrix} j_1 & j_2 & j \\ a & b & m \end{pmatrix} \begin{pmatrix} j_1 & j_2 & j \\ c & d & m \end{pmatrix} = \delta_{a,c} \delta_{b,d}, \quad (A2)$$

where  $\delta_{\alpha,\beta}$  is the Kronecker-Weierstrass symbol and equalities  $a + b + m = 0$ ,  $c + d + m = 0$  hold. Consider particular values of  $3j$ -Wigner symbols [36]:

$$\begin{pmatrix} 1 & 1 & 0 \\ a & b & 0 \end{pmatrix} = \frac{1}{\sqrt{3}} (-1)^{1+b} \delta_{a,-b}, \quad (A3)$$

$$\begin{pmatrix} 1 & 1 & 1 \\ a & b & 0 \end{pmatrix} = \frac{1}{\sqrt{6}} (-1)^b a \delta_{a,-b}, \quad (A4)$$

$$\begin{pmatrix} 1 & 1 & 1 \\ a & b & \pm 1 \end{pmatrix} = \pm \frac{1}{2\sqrt{3}} (-1)^b \sqrt{(1 \mp b)(2 \pm b)} \delta_{a, \mp 1-b}. \quad (A5)$$

Then, for  $j_1 = j_2 = 1$  and  $j = 0, 1, 2$  from (A2) we obtain

$$W_{cd}^{ab} = \frac{1}{5} \delta_{a,c} \delta_{b,d} - \frac{1}{20} (-1)^{b+d} (E + W), \quad (A6)$$

$$E = \left( 2bd + \frac{4}{3} \right) \delta_{a,-b} \delta_{c,-d}, \quad (A7)$$

$$W = W_+ + W_-, \quad (A8)$$

$$W_{\pm} = \sqrt{(1 \pm b)(2 \mp b)(1 \pm d)(2 \mp d)} \delta_{a, \pm 1-b} \delta_{c, \pm 1-d}. \quad (A9)$$

In our case (see (13) for  $Q_m$ )  $a = -M'$ ,  $b = p$ ,  $c = -M''$ ,  $d = p' = 0, \pm 1$  and  $m = M$ .

## Conflict of interest

The authors declare that they have no conflict of interest.

## References

- [1] Y. Kubota, K. Tamasaku. *Nonlinear X-Ray Spectroscopy for Materials Science* (Springer Series in Optical Science), **246**, 119–145 (2023).
- [2] M. Chergui, M. Beye, S. Mukamel, Cr. Svetina, C. Masciovecchio. *Nature Rev. Phys.*, **5**, 578 (2023). DOI: 10.1038/s42254-023-00643-7

- [3] J. Fan, J. Hofbrucker, A.V. Volotka, S. Fritzsche. Eur. Phys. J. D, **76**, 18 (2022). DOI: 10.1140/epjd/s10053-021-00334-x
- [4] A.N. Grum-Grzhimailo, E.V. Gryzlova. Phys. Rev. A, **89**, 043424 (2014). DOI: 10.1103/PhysRevA.89.043424
- [5] S.A. Novikov, A.N. Hopersky. J. Phys. B, **33**, 2287 (2000). DOI: 10.1088/0953-4075/33/12/310
- [6] S.A. Novikov, A.N. Hopersky. J. Phys. B, **34**, 4857 (2001). DOI: 10.1088/0953-4075/34/23/327
- [7] S.A. Novikov, A.N. Hopersky. Radiat. Phys. Chem., **63**, 115 (2002). DOI: 10.1016/S0969-806X(01)00225-0
- [8] S. Kühn, Ch. Cheung, N.S. Oreshkina et al. Phys. Rev. Lett., **129**, 245001 (2022). DOI: 10.1103/PhysRevLett.129.245001
- [9] Ch. Shah, M. Togawa, M. Botz et al. Astrophys. J., **969**, 52 (2024). DOI: 10.3847/1538-4357/ad454b
- [10] S.J. Gunderson, K.G. Gayley, D.P. Huenemoerder, P. Pradhan, N.A. Miller. MNRAS, **529**, 3154 (2024). DOI: 10.48550/arXiv.2206.05219
- [11] M. Nrisimhamurthy, G. Aravind, P.C. Deshmukh, S.T. Manson. Phys. Rev. A, **91**, 013404 (2015). DOI: 10.1103/PhysRevA.91.013404
- [12] L.D. Landau. Dokl. Akad. Nauk SSSR, **60**, 207 (1948).
- [13] C.N. Yang. Phys. Rev., **77**, 242 (1950). DOI: 10.1103/PhysRev.77.242
- [14] A.N. Hopersky, A.M. Nadolinsky, S.A. Novikov. Phys. Rev. A, **98**, 063424 (2018). DOI: 10.1103/PhysRevA.98.063424
- [15] N. Bloembergen. *Nonlinear Optics* (World Scientific, Singapore, 1996).
- [16] P. Lambropoulos, X. Tang. J. Opt. Soc. Am. B, **4**, 821 (1987). DOI: 10.1364/JOSAB.4.000821
- [17] R. Loudon. *The Quantum Theory of Light* (Oxford Science Publications, 2001).
- [18] A.N. Hopersky, R.V. Koneev. Bulletin of Higher Educational Institutions. North Caucasus Region. Natural Science, **1**, 24 (2023). DOI: 10.18522/1026-2237-2023-1-24-28
- [19] M.H. Chen, B. Crasemann, Kh.R. Karim, H. Mark. Phys. Rev. A, **24**, 1845 (1981). DOI: 10.1103/PhysRevA.24.1845
- [20] A. Hibbert, M. Le Dourneuf, M. Mohan. At. Data Nucl. Data Tables, **53**, 23 (1993).
- [21] T. Shirai, J. Sugar, A. Musgrove, W.L. Wiese. J. Phys. Chem. Ref. Data Monograph., **8**, 1–632 (2000). DOI: 10.1063/1.555907
- [22] C. Bostedt, J.D. Bozek, P.H. Bucksbaum et al. J. Phys. B, **46**, 164003 (2013). DOI: 10.1088/0953-4075/46/16/164003
- [23] I. Nam, Ch-K. Min, B. Oh et al. Nat. Photonics, **15**, 435 (2021). DOI: 10.1038/s41566-021-00777-z.
- [24] Ch. Grech, M.W. Guetg, G.A. Geloni et al. Phys. Rev. Accel. Beams, **27**, 050701 (2024). DOI: 10.1103/PhysRevAccelBeams.27.050701
- [25] A.A. Kryloveckij, N.L. Manakov, S.I. Marmo. ZhETF, **119**, 45 (2001) (in Russian).
- [26] B. Gao, A.F. Starace. Phys. Rev. Lett., **61**, 404 (1988). DOI: 10.1103/PhysRevLett.61.404
- [27] A.E. Orel, T.N. Rescigno. Chem. Phys. Lett., **146**, 434 (1988). DOI: 10.1016/0009-2614(88)87473-6
- [28] E.I. Staroselskaya, A.N. Grum-Grzhimailo. Moscow Univ. Phys., **70**, 374(2015). DOI: 10.3103/S0027134915050148.
- [29] A.N. Hopersky, A.M. Nadolinsky, S.A. Novikov. J. Phys. B, **57**, 215601 (2024). DOI: 10.1088/1361-6455/ad7cab
- [30] [M.Ya. Amusia. *Atomic Photoeffect* (Springer, US, 2013).
- [31] G. Breit, J.A. Wheeler. Phys. Rev., **46**, 1087 (1934). DOI: 10.1103/PhysRev.46.1087
- [32] J.D. Brandenburg, J. Seger, Z. Xu, W. Zha. Rep. Prog. Phys., **86**, 083901 (2023). arXiv:2208.14943 [hep-ph]
- [33] The STAR Collaboration. Phys. Rev. Lett., **127**, 052302 (2021). DOI: 10.1103/PhysRevLett.127.052302
- [34] The CMS Collaboration. arXiv:2412.15413v1 [nucl-ex] (2024). DOI: 10.48550/arXiv.2412.15413
- [35] D.A. Varshalovich, A.N. Moskalev, V.K. Khersonsky. *Quantum Theory of Angular Momentum* (World Scientific, Singapore, 1988).
- [36] I.I. Sobelman. *Theory of Atomic Spectra* (Alpha Science International Ltd, Oxford, 2006).

Translated by J.Savelyeva